

Physicochemical features of the formation of siliceous porous mesophases

2.* Effect of the size of the surfactant cation

V. N. Romannikov,* V. B. Fenelonov, and A. Yu. Derevyankin

G. K. Boreskov Institute of Catalysis, Siberian Branch of the Russian Academy of Sciences,
5 prosp. Akad. Lavrent'eva, 630090 Novosibirsk, Russian Federation.
Fax: +7 (383 2) 34 3056. E-mail: zeolite@catalysis.nsk.su

The formation of siliceous mesoporous mesophase materials (SiO₂-MMM) prepared by precipitation of soluble forms of SiO₂ with alkyltrimethylalkylammonium bromide C_nTMABr ($n = 12, 14, 16, 18$ is the number of carbon atoms in the alkyl chain) was investigated. An increase in the n value has no influence on the mechanism of formation of SiO₂-MMM but causes an increase in the size and volume of mesopores with the mesopore specific surface area and wall thickness remaining virtually constant.

Key words: mesophase mesoporous materials, mesoporous silicates, MCM-41, porous structure, formation of mesophase.

The main stages and the mechanism of formation of siliceous mesophase mesoporous materials (Si-MMM) of the MCM-41 type, prepared by homogeneous precipitation of SiO₂ from sodium silicate in the presence of an ionic surfactant (cetyltrimethylammonium cations, C₁₆TMA⁺) have been outlined previously.^{2,3} The reaction between the components at room temperature affords the primary mesophase as a result of self-assembling of low-molecular-weight SiO₂-based anionic species and surfactant cations. Annealing of the primary mesophase in air at 550–580 °C yields a highly porous product with nanosized mesopores but with an insufficiently ordered structure. Hydrothermal treatment (HTT) of the primary mesophase in the mother liquor at 120 °C enables higher structural ordering, apparently, due to the thermal motion and expansion of the hydrocarbon moieties of the surfactant cations. The expansion leads to an increase in the hexagonal lattice parameter accompanied by a corresponding increase in the dimensions and volume of the pores arising after the removal of the surfactant.

In this work, SiO₂-MMM were synthesized under conditions described in the previous communication¹ but using alkyltrimethylammonium cations C_nTMA⁺ containing $n = 12, 14, 16$, or 18 carbon atoms in the alkyl chain. The purpose of this study was to elucidate the possible influence of the length of the alkyl chain in the surfactant on the mechanism and stages of formation of SiO₂-MMM.

Experimental

The SiO₂-MMM were prepared (see Ref. 1) by homogeneous precipitation of SiO₂ from a solution of sodium silicate in the presence of C_nH_{2n+1}Me₃NBr ($n = 12, 14, 16, 18$) at a

fixed molar ratio of the components in the reaction mixture, SiO₂ : 0.3 C_nTMABr : 0.3 NaOH : 102 H₂O, at room temperature followed by HTT at 120 ± 5 °C. The pH value was 10.5–11.5 in all cases. The duration of HTT (τ_{HTT}) varied from 0 to 404 h. Then the precipitates were filtered off, washed with warm water, dried at 30–40 °C, and annealed in air at 550–580 °C. The resulting SiO₂-MMM samples were designated by symbols C n - τ_{HTT} (where n is the number of carbon atoms in the alkyl chain; τ_{HTT}/h is the duration of HTT). The index C n -0 corresponds to the *primary mesophases* obtained by precipitation of the components at room temperature without HTT ($\tau_{\text{HTT}} = 0$).

As in the previous study,¹ the molar ratio $M_R = \text{NR}_4^+/\text{SiO}_2$ was calculated for dried samples. The structures of dried and annealed SiO₂-MMM samples were studied by powder X-ray diffraction analysis for the 1–7° 2 θ using a URD-63 diffractometer. Primary attention was paid to the (100), (110), (200), and (210) reflexes, which are characteristic of a mesophase with a hexagonal structure, and to the half-width of the most intense diffraction reflex, (100), expressed in terms of the Bragg angles 2 θ . These reflexes were used to calculate the hexagonal unit cell parameter a_0 ; the (100) reflex half-width (below referred to as B_{100}) was regarded as a characteristic of the degree of ordering of the pore lattice.¹ Diffraction measurements were carried out at a rate of 0.5 deg min^{−1}, which ensured a reproducibility of the a_0 values sufficient for comparison of the samples (at least ±0.1 nm). Data for the C16 series were obtained under the same conditions, which permitted comparison of the results of this study with those obtained previously.¹

The texture of annealed SiO₂-MMM samples was studied based on N₂ adsorption isotherms, which were obtained at 77 K on an ASAP-2400 instrument and used to calculate the specific surface area A_{me} and the volume V_{me} of mesopores in the mesophase particles and also the total specific surface area of the amorphous phase and the external surface area of the mesophase particles, A_{ext} ($A_{\text{BET}} \approx A_{\text{me}} + A_{\text{ext}}$). The A_{me} , V_{me} , and A_{ext} values were calculated by a procedure based on the comparison method (i.e., comparison of the experimental adsorption isotherm with that measured on a nonporous surface

* For Part 1, see Ref. 1.

under the same conditions), which had been described in detail.⁴⁻⁶ The size of mesopores d_{me} and the characteristic thickness of the walls between them h_w were estimated using the relations⁴⁻⁶ of the model of hexagonal packing of coaxial cylindrical mesopores. In this model, the hexagonal lattice parameter $a_0 = d_{me} + h_w$, and d_{me} is related to a_0 and to the bulk porosity of the mesophase ε_{me} as follows:

$$d_{me} = a_0 \sqrt{\frac{2\sqrt{3}}{\pi} \varepsilon_{me}} \approx 1.05 a_0 \sqrt{\varepsilon_{me}}, \quad (1)$$

where

$$\varepsilon_{me} = \frac{V_{me}\rho}{V_{me}\rho + 1}, \quad (2)$$

ρ is the mesophase density measured by helium at room temperature on an Autopycnometer 1320 instrument, and V_{me} is the specific volume of the mesopores calculated from the adsorption isotherms using published data.⁴

The results of MAS ²⁹Si NMR spectroscopy studies of the C16 series obtained on a Bruker MSL-400 spectrometer (79.49 MHz) were used.

Results and Discussion

The shape of the isotherms (Figs. 1 and 2) is normal for SiO₂-MMM¹⁻⁷ and allows one to distinguish three typical regions: region I corresponding to low relative pressures of nitrogen p/p_0 , in which adsorption occurs on the whole accessible surface, region II in which the adsorbed amount increases stepwise upon small changes in p/p_0 and which corresponds to the filling of mesopores in the bulk of the mesophase particles, and region III located at great p/p_0 values, in which adsorption continues on the surface having remained free after coverage of the mesopores in the mesophase bulk.

These regions are displayed more clearly when these isotherms are represented as comparative plots, i.e., plots representing the adsorbed amount $\alpha(p/p_0)$ for the isotherm studied vs the amount adsorbed on a reference nonporous specimen $\alpha(p/p_0)$ at the same p/p_0 value (for the sake of convenience of the subsequent analysis, the $\alpha(p/p_0)$ values are related to unit surface). Examples of these comparative plots are shown in Fig. 3; the use of these plots for the analysis of the texture of MMM was substantiated in detail previously⁴; a similar strategy was used in some other studies.⁵⁻⁷ In these plots, region I of the isotherm is described by a linear dependence that can be extrapolated to the origin. This implies the absence of micropores, and the slope of the plots in this region corresponds to the total specific surface area $A_{BET} \approx (A_{me} + A_{ext})$, where A_{BET} is the surface area calculated by the BET method. Region III of the isotherm is also described by a linear dependence, whose slope corresponds to the A_{ext} value and the intercept obtained by extrapolation to the ordinate axis makes it possible to determine the mesopore volume V_{me} . The average mesopore dimension d_{me} was calculated by Eqs. (1) and (2) using the mesopore volume V_{me} , the density ρ_{He} , and the hexagonal lattice parameter a_0 found from

the diffraction measurements. It has been shown⁴⁻⁶ that this calculation method is more favorable than the generally accepted methods commonly used to calculate the pore size in MMM, which are based on various modifications of the Kelvin equation and other equations relating the pore size to the p/p_0 value. The length of the section corresponding to the filling of mesopores along the p/p_0 axis is an indicator of the homogeneity of the mesopore sizes.

It can be seen from Fig. 1 that the isotherm of N₂ adsorption on the annealed primary mesophase has a shape typical of MMM; however, the relatively large region II, in which the mesopores are filled, points to nonuniformity of their sizes. Even a short-term HTT increases the uniformity, which subsequently hardly de-

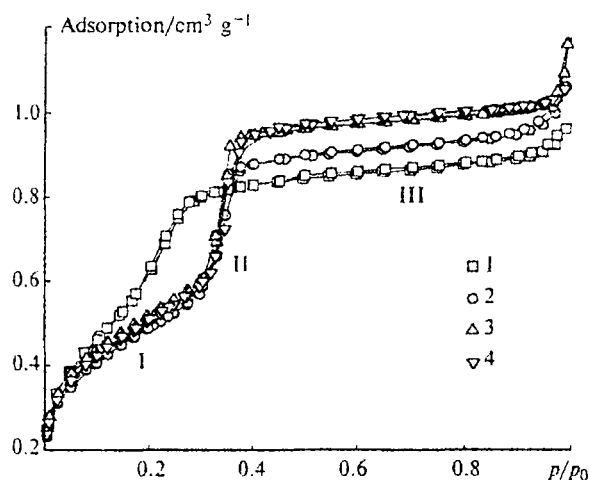


Fig. 1. Nitrogen adsorption isotherms for samples of the C16 series at various HTT times (τ_{HTT}): 1, C16-0; 2, C16-7; 3, C16-64; 4, C16-404. I–III are characteristic regions of isotherms.

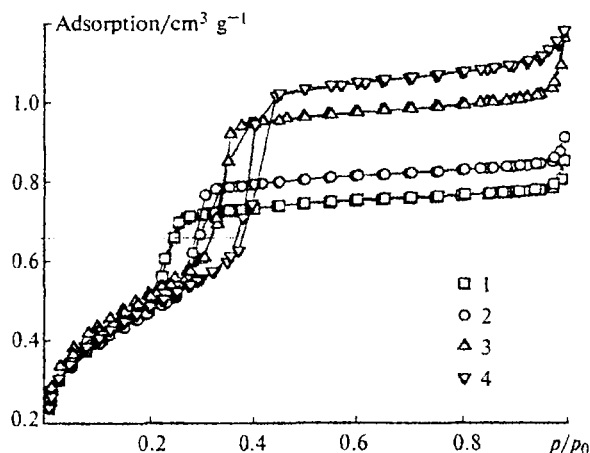


Fig. 2. Nitrogen adsorption isotherms for samples of various series at identical HTT times ($\tau_{HTT} = 64$ h): 1, C12-64; 2, C14-64; 3, C16-64; 4, C18-64.

depends on τ_{HTT} . This effect can be reproduced for all of the series studied. For illustration, Table 1 shows the values for the relative N_2 pressure, p/p_0 , corresponding to the beginning $(p/p_0)_b$ and to the end $(p/p_0)_e$ of the mesopore filling section and those estimated from the adsorption isotherms for characteristic samples.

It follows from Fig. 2 that an increase in the parameter n is accompanied by an increase in the size and volume of mesopores without substantial changes in the initial sections of the isotherms corresponding to the adsorption over the whole accessible surface. The results of quantitative analysis of the N_2 adsorption isotherms are listed in Table 2, which summarizes the most important data obtained by various experimental and calculation methods.

Comparison of the results obtained for different series allows one to conclude that the number of carbon

atoms n in the alkyl chain most appreciably affects the hexagonal unit cell parameter a_0 as well as the size d_{me} and the volume V_{me} of mesopores. This is a consequence of the shape-forming role of the surfactant in the mechanism of mesophase formation.^{2,3} It can also be noted that the rates of variation of the structural characteristics recorded in the X-ray diffraction analysis are somewhat different in various series; the annealed samples of the C14 and C16 series obtained without HTT exhibit three characteristic reflexes and those after HTT are responsible for four reflexes. In the C12 and C18 series, three reflexes can be observed only at $\tau_{\text{HTT}} > 40$ h and $\tau_{\text{HTT}} > 3$ –5 h, respectively. These differences may be due to the fact that in the procedure used to prepare the samples, the initial components were taken at a fixed molar ratio, which corresponded to different volume ratios; apparently, the latter value in the C14 and C16 series was more favorable.

The density ρ_{He} of the annealed samples is 2.33 ± 0.04 g cm^{-3} in the C12 series, 2.26 ± 0.04 g cm^{-3} in the C14 series, 2.13 ± 0.04 g cm^{-3} in the C16 series, and 2.03 ± 0.04 g cm^{-3} in the C18 series. However, the insufficient accuracy of the measurements, which is due to the small size of samples, did not allow us to elucidate any obvious correlation between ρ_{He} and τ_{HTT} , whereas the tendency found for a dependence of ρ_{He} on the size of surfactant molecules requires additional evidence. All the ρ_{He} values determined are in the range typical of amorphous SiO_2 forms.⁸

The evolution of all the other parameters presented in Table 2 within each series is qualitatively similar to that described previously¹ for the C16 series. In fact, the thermally stable *primary* mesophase is formed in all cases even at room temperature and possesses properties similar within each series, namely, relatively low ordering (the maximum values for the structural parameter $B(d_{100})$ and for the length of section II on the isotherm), minimum values for the parameter a_0 and the mesopore volume and size, and close values for the calculated thickness of the mesopore wall h_w , the total specific surface area and the surface area of mesopores, and the molar ratio $M_R = \text{NR}_4^+/\text{SiO}_2$.

The thermal expansion of the surfactant micelles at the initial stage of HTT is always accompanied by a discontinuous increase in the a_0 parameter and the volume V_{me} and size d_{me} of mesopores. This is accompanied by a decrease in the mesopore specific surface area A_{me} and the total surface area, the $M_R = \text{NR}_4^+/\text{SiO}_2$ and $B(d_{100})$ values, and the length of the section of mesopore filling on the adsorption isotherms (see Table 1). As τ_{HTT} increases, these parameters change insignificantly and more monotonically or remain virtually constant. Thus, the mesopore specific surface areas A_{me} for all of the samples remain at a level of 1050 ± 65 m² g⁻¹, the total specific surface area is $A_{\text{me}} + A_{\text{ext}} \approx 1110 \pm 30$ m² g⁻¹, and the calculated thickness of the mesopore walls $h_w \approx 0.65 \pm 0.05$ nm. The mesopore

Table 1. Width of the range of mesopore filling on N_2 adsorption isotherms at 77 K

Sample	$(p/p_0)_b$	$(p/p_0)_e$	$\Delta(p/p_0)$
C12-0	0.107	0.204	0.097
C12-404	0.196	0.278	0.082
C14-0	0.096	0.224	0.128
C14-404	0.248	0.306	0.058
C16-0	0.169	0.236	0.169
C16-404	0.305	0.375	0.070
C18-0	0.280	0.377	0.097
C18-404	0.355	0.404	0.050

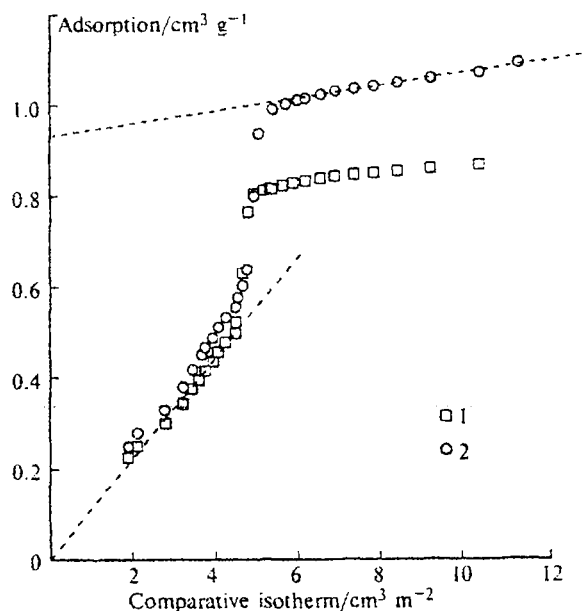


Fig. 3. Examples of comparative plots for C14-64 (1) and C16-64 (2).

Table 2. Main experimental and theoretical results

Sample	After drying		After annealing					
	M_R	a_0 /nm	$B(d_{100})$ /deg	A_{me} $m^2 g^{-1}$	A_{ext} $m^2 g^{-1}$	V_{me} $/cm^3 g^{-1}$	d_{me} nm	H_w
C12-0	0.22	3.53	0.95	1201	50	0.64	2.46	0.59
C12-3	0.19	3.85	0.62	1015	79	0.73	3.06	0.61
C12-7	0.17	3.85	0.66	1022	74	0.76	3.11	0.59
C12-20	0.17	3.97	0.61	1038	47	0.76	3.16	0.61
C12-64	0.16	3.95	0.47	1090	38	0.73	3.18	0.63
C12-188	0.17	3.81	0.33	1041	37	0.78	3.19	0.59
C12-404	0.16	3.85	0.22	1046	43	0.76	3.20	0.61
C14-0	0.22	3.81	0.52	1139	114	0.66	2.55	0.57
C14-3	0.20	4.27	0.27	990	64	0.77	3.34	0.65
C14-7	0.19	4.22	0.18	1064	62	0.80	3.38	0.63
C14-20	0.19	4.36	0.19	995	59	0.81	3.44	0.64
C14-64	0.19	4.27	0.19	1000	44	0.79	3.48	0.66
C14-188	0.19	4.33	0.18	1078	45	0.85	3.56	0.63
C14-404	0.19	4.29	0.20	1109	30	0.87	3.62	0.62
C16-0	0.25	4.17	0.41	1173	82	0.81	2.96	0.58
C16-3	0.21	4.59	0.23	993	90	0.82	3.62	0.70
C16-7	0.20	4.47	0.26	984	99	0.85	3.70	0.69
C16-20	0.20	4.56	0.24	1083	84	0.88	3.79	0.68
C16-64	0.20	4.53	0.22	1107	64	0.94	3.80	0.63
C16-188	0.20	4.66	0.22	1105	36	0.94	3.87	0.64
C16-404	0.19	4.70	0.22	1114	57	0.95	3.97	0.65
C18-0	0.27	4.61	0.52	1142	95	1.01	3.44	0.56
C18-3	0.24	4.90	0.33	1026	140	1.01	3.81	0.62
C18-7	0.23	4.80	0.39	1002	112	0.99	3.84	0.64
C18-20	0.23	4.82	0.30	1042	103	1.02	3.92	0.63
C18-64	0.21	4.70	0.34	1016	89	1.00	3.95	0.65
C18-188	0.22	4.82	0.34	1048	80	1.04	4.11	0.64
C18-404	0.22	4.82	0.41	1026	101	1.01	4.10	0.66

volume V_{me} either virtually does not change (the C12 and C18 series) or slightly increases (the C14 and C16 series) with an increase in τ_{HTT} . The $h_w \approx 0.65 \pm 0.05$ nm value is close to the double size of the $[SiO_4]$ tetrahedron.

When τ_{HTT} increases, the a_0 and d_{me} values and the degree of ordering (decrease in $B(d_{100})$) tend to increase at $h_w \approx \text{const}$, which is typical of annealed samples. In addition, an increase in τ_{HTT} is accompanied by a decrease in the relative linear shrinkage upon annealing, which can be estimated as $\lambda = (a_{0d} - a_{0a}) \cdot 100/a_{0d}$, where a_{0d} and a_{0a} are the values of the a_0 parameter for dry and annealed samples, respectively. The λ values for primary mesophases vary from 13 to 17%; they decrease to 5–8% for $\tau_{HTT} = 3$ h and to 1–2% for $\tau_{HTT} = 404$ h.

According to a known publication,⁹ the decrease in a_0 upon annealing is due to polycondensation of SiO_2 , which continues at this stage. This was detected⁹ by MAS ^{29}Si NMR spectroscopy based on the increase in the proportion of silicon atoms in the high-coordinate Q_4 state, in which each Si atom is bound *via* oxygen bridges to four Si atoms to form $Si(OSi)_4$ groups. Let us make some estimates using the MAS ^{29}Si NMR data for

the C16 series reported previously.¹ The annealed samples of this series contain 54–59% of silicon atoms in the Q_4 state; the proportion of the Q_4 states in dried samples is ~33% for C16-0, ~43% for C16-3, and ~52% for C16-404. Thus, annealing of the primary C16-0 mesophase is accompanied by a ~1.7-fold increase in the Q_4 value ($\lambda \sim 15\%$); in the case of C16-3, the Q_4 values increase ~1.3-fold ($\lambda \sim 5.8\%$), and for C16-404, they increase by a factor of ~1.1 ($\lambda \sim 2\%$). The relative variations in the Q_4 and a_0 parameters are clearly correlated (correlation coefficient 0.999). Therefore, the tendency of the parameter a_0 and the mesopore size and volume to increase with an increase in τ_{HTT} can be due to the fact that processes of SiO_2 polycondensation continue during the HTT and this decreases the degree of shrinkage upon annealing.

This shrinkage is the most pronounced for the primary mesophase and, apparently, it additionally increases the degree of disorder in the annealed forms. In this connection, some correlation can be noted between the λ and $B(d_{100})$ parameters for samples having been subjected to HTT; this can also be associated with the nonuniform shrinkage during annealing. Therefore, the degree of shrinkage during annealing is among the fac-

tors that influence the structure and texture of MMM. As a consequence, the size of mesopores d_{me} in SiO₂-MMM is determined by not only the length of the hydrocarbon chain in the surfactant cations and their thermal expansion but also by the polycondensation processes during the HTT.

The results obtained indicate that all of the studied systems display a qualitatively similar behavior at the stages of formation of the primary mesophase, hydrothermal treatment, and annealing. This suggests that under the synthesis conditions employed, the main stages and the mechanism of formation of the SiO₂ mesophase involving a surfactant of the C_nTMA⁺ type with 12 to 18 carbon atoms n in the alkyl chain depend only slightly, in the first approximation, on the length of the alkyl chain.

This work was financially supported by the Russian Foundation for Basic Research (Project No. 98-03-32390a).

References

1. V. N. Romannikov, V. B. Fenelonov, A. Nosov, V. Yu. Derevyankin, S. Tsybulya, and G. N. Kryukova, *Izv. Akad. Nauk, Ser. Khim.*, 1999, 1845 [*Russ. Chem. Bull.*, 1999, **48**, 1821 (Eng. transl.)].
2. C. T. Kresge, M. E. Leonowicz, W. J. Roth, J. C. Vartuli, and J. S. Beck, *Nature* (London), 1992, **359**, 710.
3. J. S. Beck, J. C. Vartuli, W. J. Roth, M. E. Leonowicz, C. T. Kresge, K. D. Schmitt, C. T.-W. Chu, D. H. Olson, E. W. Sheppard, S. B. McCullen, J. B. Higgins, and J. I. Schlenker, *J. Am. Chem. Soc.*, 1992, **114**, 10634.
4. V. B. Fenelonov, V. N. Romannikov, and A. Yu. Derevyankin, *Microporous Mesoporous Materials*, 1999, **28**, 57.
5. M. Kruk, M. Jaroniec, and A. Sayari, *Langmuir*, 1997, **13**, 6267.
6. M. Kruk, M. Jaroniec, R. Ruoo and J. M. Kim, *Microporous Mater.*, 1997, **12**, 93.
7. P. J. Branton, P. G. Hall, and K. S. W. Sing, *J. Chem. Soc., Chem Commun.*, 1993, 1257.
8. R. Iler, *The Chemistry of Silica*, Wiley, New York, 1979.
9. Chi-Feng Cheng, Dong Ho Park, and J. Klinowski, *J. Chem. Soc., Faraday Trans.*, 1997, **93**, 193.

Received December 3, 1998